PAPER

Check for updates

Flame retardancy and wear resistance of epoxy composites modified by whisker-shaped nickel phyllosilicate and microencapsulated ammonium polyphosphate

Shibin Nie, [ID] *[ad] Wenli Zhai, [ID] [b] Yuxuan Xu, [ID] [b] Wei He[b] and Jinian Yang[c]

Whisker-shaped nickel phyllosilicate (NiPS) was synthesized using rod-like nickel-based metal–organic frameworks as the hard templates, and highly efficient flame retardant and wear resistant EP composites were prepared by synergizing with microencapsulated ammonium polyphosphate (MFAPP). The research results indicated that at a total addition amount of 8 wt% and a mass ratio of 2 : 5 for NiPS to MFAPP, the limiting oxygen index of the EP composite was 28.2%, which achieved the V-0 rating in the UL-94 standard. Meanwhile, the peak of heat release rate and total heat release was reduced by 33.9% and 22%, respectively, compared with pure EP. The synergistic system of NiPS and MFAPP promoted the formation of high-quality char layer, preventing the diffusion of heat, oxygen, and combustible gases effectively during combustion of the EP composite. Dry friction test showed that the wear rate of the EP composite was 0.847×10^{-5} mm^3 N^{-1} m^{-1}, which was 87.9% lower than pure EP, indicating a significant improvement in wear resistance. This study provided a promising method for the preparation of high performance epoxy composites with excellent flame retardancy and wear resistance.

1. Introduction

As one of the most important thermosetting polymers, epoxy resin (EP) is widely used in electronics, construction, coating, aerospace and other fields due to excellent bonding strength, electrical insulation, sealing properties and outstanding mechanical performance. However, its flammability and release of toxic gases such as carbon monoxide during combustion limit its application in areas with high fire safety requirements greatly.[1–3] Additionally, the three-dimensional cross-linked network structure of EP also results in poor tribological properties relatively, restricting the development in the field of friction components.[4,5] Therefore, in order to broaden application field, it is of great practical significance to develop high performance EP composites with excellent flame retardancy and friction performances.

Introducing nanoscale inorganic fillers is a direct and effective strategy to endow polymers with excellent comprehensive properties, and they can exhibit improved performance significantly at low contents.[6,7] Li *et al.* developed a biobased

modification of Mg–Al layered double hydroxide using a derivative of eugenol, the addition of 8 wt% of this modifier can achieve a UL-94 flame retardant rating of V-0 for epoxy resin.[8] Wang *et al.* functionalized DBS-LDH with SiO$_2$ using an electrostatic self-assembly method to obtain DBS-LDH@silica nanomaterials, which have excellent self-extinguishing properties at an addition of 3 wt%.[9] Wang found that the addition of 5 wt% Ni@NiO reduced the wear rate of EP by a factor of 22.2.[10] Song found that the addition of KH550-modified nano BN can improve the mechanical properties, thermal stability, and friction-wear performance of EP effectively.[11] Most researchers tend to focus on the modification of EP for a single property, and the multifunctional modification integrating flame retardancy and wear resistance are rarely mentioned.

Nickel phyllosilicate is a hydrous silicate, composed of silica–oxygen tetrahedra interconnected by sharing 3/4 corner tops to form two-dimensional wirelessly extended silica–oxygen tetrahedral layers, which are categorized into 1 : 1 and 2 : 1 types based on the lamellar structure.[12] High purity nickel phyllosilicate is usually synthesized using silicon and nickel ions. As a two-dimensional nanomaterial, nickel phyllosilicate exhibits characteristics such as regular and ordered layer structure, high specific surface area, and designability of inorganic/organic functional groups.[13] In previous work, various kinds of nickel phyllosilicate and their derivatives including organically modified nickel phyllosilicate, flower-like phyllosilicate, whisker-shaped nickel phyllosilicate, *etc.* have been synthesized

aSchool of Public Security and Emergency Management, Anhui University of Science and Technology, Hefei 231131, P. R. China. E-mail: nieshibin88@163.com

bSchool of Safety Science and Engineering, Anhui University of Science and Technology, Huainan 232001, P. R. China

cSchool of Materials Science and Engineering, Anhui University of Science and Technology, Huainan 232001, P. R. China

dInstitute of Energy, Hefei Comprehensive National Science Center, Hefei, 230051, P. R. China

successfully. Among them, whisker-shaped nickel phyllosilicates (NiPS) is synthesized by reacting rod-like metal–organic frameworks (Ni-MOF) containing nickel ions as templates with caustic soda (NaOH) as a mineralizer under hydrothermal conditions. NiPS maintain a relatively uniform dispersion state in the EP matrix. NiPS can improve the wear resistance of EP effectively, the introduction of only 1 wt% of filler can reduce the wear rate by 80%, compared to pure EP. Adding 5 wt% NiPS can increase the LOI value of EP from 23.8% to 27.1% and suppress the generation of molten droplets effectively. However, the combustion time only decreases from approximately 224 s to 113 s, without achieving any flame retardant rating.[14]

In order to further enhance the flame retardancy and wear resistance of EP composites, NiPS was synthesized using Ni-MOFs as the hard templates by facile hydrothermal method, and selected to form a synergistic system with micro-encapsulated ammonium polyphosphate (MFAPP) in this paper. MFAPP has good flame retardant properties, and the surface is very smooth after microencapsulation with diamine resin (MF). By studying the influence of MFAPP and NiPS on the flame retardant and friction properties of EP systematically, high-efficiency flame retardant and wear-resistant EP composites were prepared.

2. Experimental

2.1. Materials

Nickel nitrate hexahydrate ($Ni(NO_3)_2 \cdot 6H_2O$, ≥98%), NaOH (96%), sodium metasilicate nonahydrate ($Na_2SiO_3 \cdot 9H_2O$, ≥98%), and ammonia monohydrate ($NH_3 \cdot H_2O$, 25–28%) were purchased from Sinopharm Chemical Reagent Co., Ltd, China. Benzene-1,3,5-tricarboxylic acid (BTC, 99%), 4,4′-diaminodiphenylmethane (DDM, 97%) and glacial acetic acid (99.9%) were purchased from Shanghai Aladdin Industrial Corporation, China. Anhydrous ethanol (99.7%) and acetone (99.5%) were from Shanghai Titan Science Company. Formaldehyde solution (37%) was purchased from Yantai Shuanghuang Chemical Co., Ltd. Ammonium polyphosphate (APP, type II, degree of polymerization > 1000) was supplied by Xingxing Flame Retardant Co., Ltd, Zhenjiang, China. Bisphenol A diglycidyl ether (DGEBA, E-51, industrial) was purchased from Blue Star New Materials Co., Ltd., with the epoxide value of 0.48–0.53 mol 100 g^{-1}. Deionized water was produced in our lab.

2.2. Preparation of NiPS whiskers

The NiPS were prepared by a simple hydrothermal method based on our previous study.[14] 1.14 g of Na_2SiO_3 was dissolved in 60 mL of deionized water, and 0.8 g of Ni-MOF was dissolved in 60 mL of ethanol–water mixture. The two solutions were mixed and stirred for 15 min, 6 mL of 1 mol per L NaOH solution was added dropwise during the stirring process. Then the mixture was subjected to ultrasonication for 30 min to prevent aggregation. The resulted suspension was transferred to a reaction Teflon-lined stainless autoclave and reacted at 160 °C for 15 h. The autoclave was left to cool naturally to room temperature, and then the green product recognized as NiPS whiskers were collected by centrifugation at 3000 rpm for 5 min, washed multiple times with a deionized water–alcohol solution and dried at 70 °C.

2.3. Preparation of EP composites

A certain amount of DGEBA was weighed and stirred in a water bath at 75 °C. NiPS and MFAPP were added to 20 mL of acetone solution, sonicated for 30 min, and then added to the epoxy suspension. DDM was heated at 100 °C for 4 h, then poured into the epoxy mixture and stirred for 5 min. Finally, the mixture was cured at 100 °C and 150 °C for 2 h each in a vacuum oven. The specific formulation is shown in Table 1.

2.4. Characterization

The surface morphology of samples were characterized using scanning electron microscopes (SIGMA-500, Carl Zeiss AG, Germany), transmission electron microscopy (JEOL-2010, Shimadzu Corporation, Japan) and energy dispersive X-ray spectroscopic mapping (Shimadzu Corporation, Japan). The limiting oxygen index (LOI) was calculated using a TTech-GBT2406 oxygen index meter (Taisi Testing Instrument Technology, China), in accordance with GB/T 2408-2021 (127 mm × 6.5 mm × 3.2 mm). The UL-94 vertical burning performance of the samples was tested using a CFZ-2-type apparatus vertical (Jiangning Analytical Instrument, China), following the GB/T 2408-2021 (127 mm × 12.7 mm × 3.2 mm). Cone calorimeter test (CCT) was measured by a cone calorimeter (FTT, the United Kingdom) following the ISO-5660 specification (100 × 100 × 3 mm), and the incident flux was 50 kW m^{-2}. Raman (HORIBA, France) spectroscopy was performed with a Renishaw inVia Raman spectrometer. TGA was tested using a TGA/SDTA851e thermoanalyzer apparatus (Mettler-Toledo, Switzerland) under a nitrogen atmosphere, and the heating rate was 10 °C min^{-1}. Thermogravimetric infrared spectrometry (TG-IR) was performed using a TGA/SDTA851e thermogravimetric analyzer combined with a Nicolet iS20 FTIR spectrophotometer under the nitrogen flow of 50 mL min^{-1}, and each sample was tested from 30 °C to 700 °C (Mettler-Toledo, Switzerland). The

Table 1 The formulations of the EP composites

Composition (wt%)	Pure EP	EP/7MFAPP	EP/7NiPS	EP/6MFAPP/1NiPS	EP/5MFAPP/2NiPS	EP/4MFAPP/3NiPS	EP/5.7MFAPP/2.3NiPS
EP	79.49	73.93	73.93	73.93	73.93	73.93	73.13
DDM	20.51	19.07	19.07	19.07	19.07	19.07	18.87
NiPS	0	0	7	1	2	3	5.7
MFAPP	0	7	0	6	5	4	2.3

tribological property under dry sliding was tested using a block-on-ring friction-testing machine (M-200, Zhonglu, China), the specific process has been well described in our previous investigation.[15] The tensile test was carried out in accordance with GB/T 1040.1-2006 using a KQL WDW-50 universal testing machine (Xinsansi, China) at room temperature with a fixed crosshead speed of 2 mm min^{-1}. The specimens used were of type 1 BA with a gauge length of 25 mm. At least 5 specimens were tested for each type.

3. Results and discussion

3.1. Microscopic characterization

SEM was used to study the surface morphology of APP and MFAPP, as shown in Fig. 1. It can be observed that the APP particles are irregular cubic solids with a rough surface and some cracks. After microencapsulation, the MFAPP particles become spherical solids with a smooth surface, and the edges and corners are relatively blurred. This significant morphological change indicates that the MF resin covers the APP particles effectively.[16] From Fig. 1(c and d), it can be seen that NiPS exhibits a rod-like morphology, composed of numerous loosely structured nanosheets, with a relatively rough surface. As shown in Fig. 1d, the high-resolution transmission electron microscopy (TEM) image of NiPS shows that the surface of NiPS consists of many nanosheets, confirming its unique layered structure. These layers are formed through an *in situ* chemical reaction and recrystallization process during hydrothermal

Table 2 The results of the LOI and UL-94 vertical burning test of EP composites^a

Samples	LOI (%)	UL-94				
		t_1	t_2	$t_1 + t_2$	Rating	Melt dropping
Pure EP	23.5	109	70	179	NR	Yes
EP/7MFAPP	27.0	31	4	35	NR	No
EP/7NiPS	24.5	82	20	102	NR	No
EP/6MFAPP/1NiPS	27.3	29	3	32	V-1	No
EP/5MFAPP/2NiPS	27.5	23	2	25	V-1	No
EP/4MFAPP/3NiPS	26.4	34	4	38	NR	No
EP/5.7MFAPP/2.3NiPS	28.2	8	1	9	V-0	No

^{a} NR mean does not meet any combustion rating.

synthesis, with an basal spacing ranging from 1.34 to 1.63 nm.[14] The high angle annular dark-field (HAADF) image and mapping results, as shown in Fig. 1f, demonstrating the uniform distribution of major elements such as Ni, O, and Si within the rod-like framework, further confirming the successful preparation of whisker-shaped nickel phyllosilicate.

3.2. Flame retardancy of EP composites

The results of UL-94 vertical burning and LOI tests of EP composites are shown in Table 2. The LOI value of the pure EP is only 23.5%, which is highly combustible and accompanied by intense flame and melt drops in the UL-94 test, with a burning
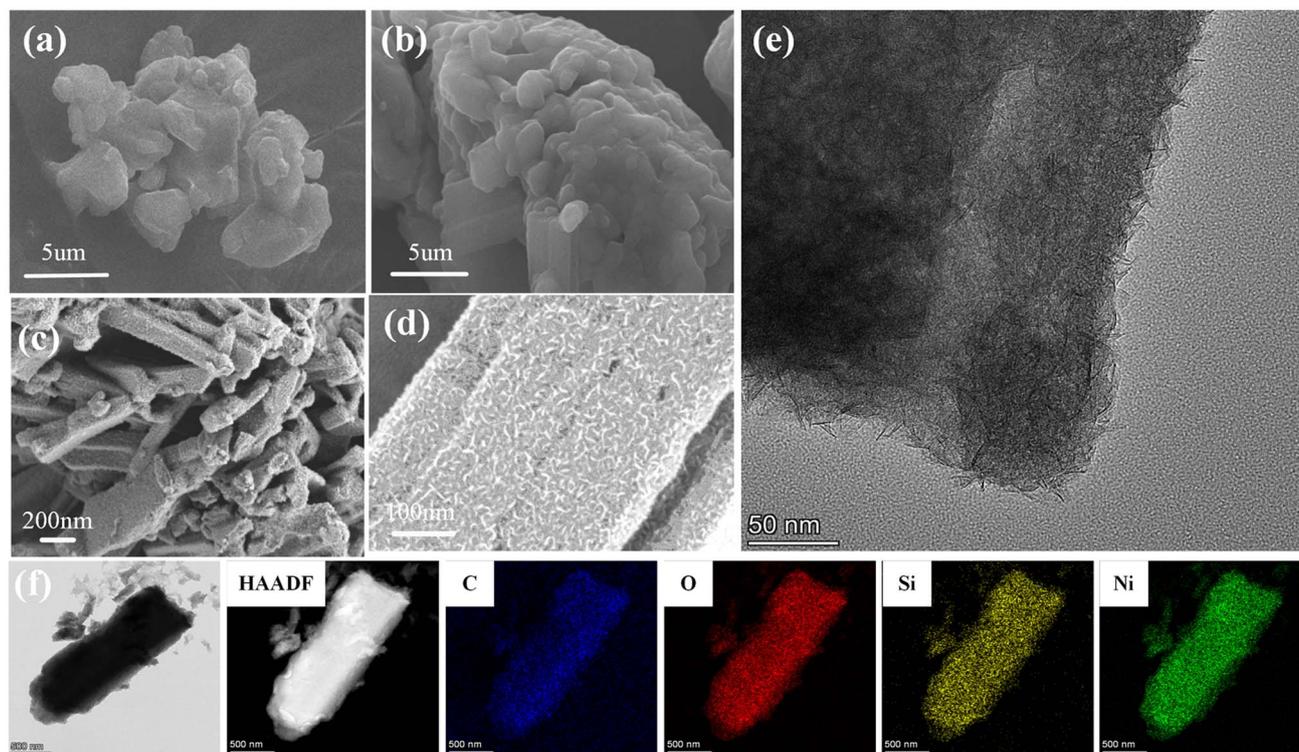

Fig. 1 SEM morphology of (a) APP, (b) MFAPP, (c and d) NiPS whiskers, (e) TEM morphology of NiPS whiskers, and (f) elemental mapping of an individual NiPS.

time of 179 s. With the addition of MFAPP or NiPS, the LOI of EP composites show different degrees of increase, and no melt drops are generated during the burning process. Under the condition of keeping 7 wt% of total addition, the LOI value of EP composites is 27% when MFAPP is added alone, and the total burning time is 35 s, which does not reach UL-94 grade. The LOI value of EP composite is 24.5% when NiPS is added alone, and the burning time was up to 102 s. The synergistic effect of MFAPP and NiPS exhibits better flame retardancy compared to the addition of MFAPP or NiPS. When the mass ratio of MFAPP to NiPS is 6 : 1, the LOI value of EP/6MFAPP/1NiPS is 27.3% and the total burning time is 32 s. When the mass ratio of MFAPP to NiPS is 5 : 2, EP/5MFAPP/2NiPS is 27.5% and the total burning time is reduced to 23 s. However, the performance of the flame retardant system decreases when the addition of NiPS is increased to 3 wt%, with an LOI value of 26.4%, which can not achieve any UL-94 rating. Above all, when the ratio of MFAPP to NiPS is 5 : 2, the EP composite has the best flame retardant effect. Under the best conditions of MFAPP and NiPS, when the total addition amount is 8 wt%, the LOI value of EP composite can reach 28.2% and pass UL-94 V-0 level, showing excellent flame retardant performance.

Cone calorimeter is one of the effective test devices used to characterize the flame retardant properties of materials widely,
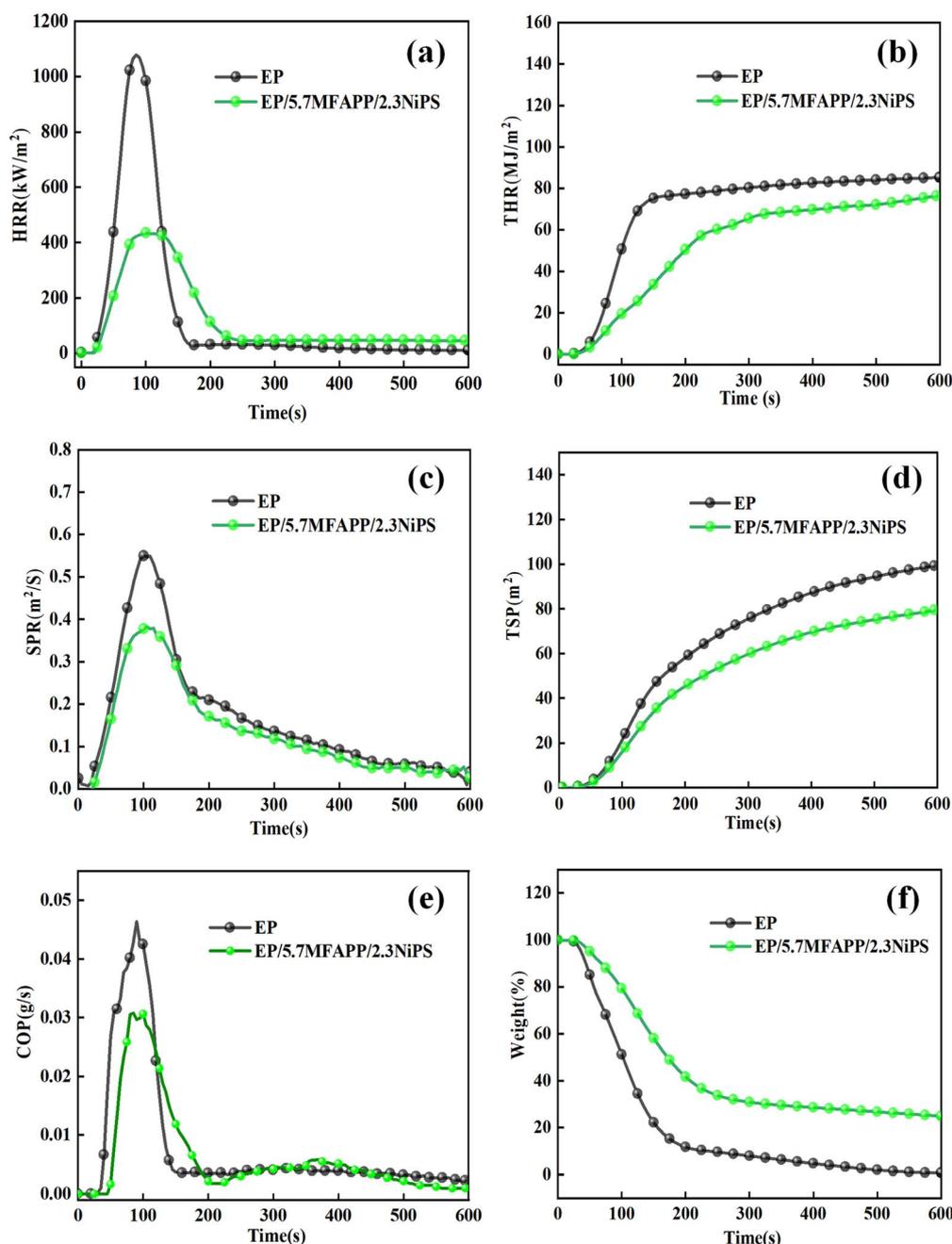

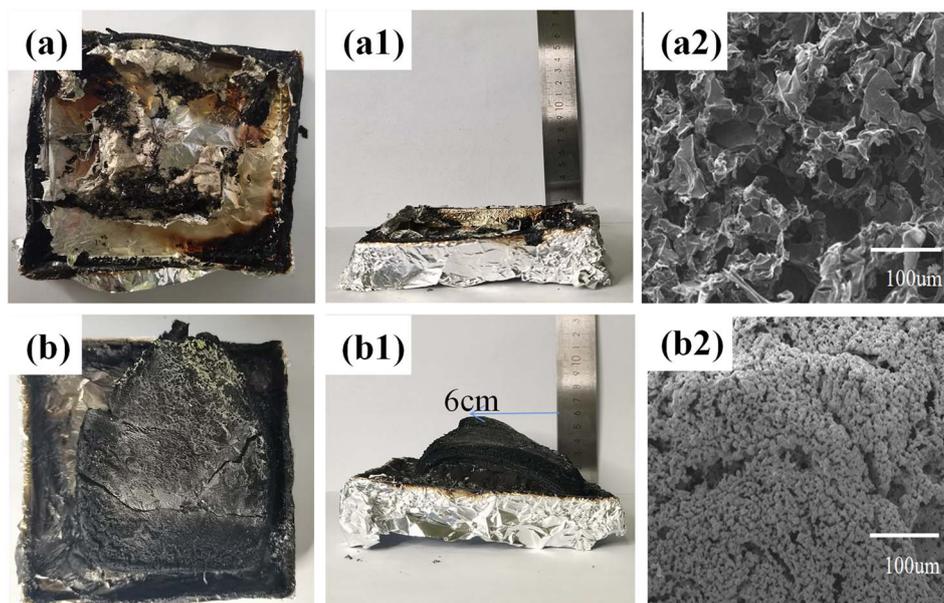Fig. 2 (a) HRR, (b) THR, (c) SPR, (d) TSP, (e) COP and (f) weight of EP composites.

Fig. 3 The digital photos and SEM of the residual char ((a–a2) EP; (b–b2) EP/5.7MFAPP/2.3NiPS).

and can reflect the actual combustion of composites.[17] Fig. 2 shows the graphs of HRR, THR, *etc. versus* time for pure EP and EP composites. The PHRR and THR of EP composite are reduced to 431 kW m^{-2} and 76.3 MJ m^{-2} after adding 8 wt% of MFAPP and NiPS to the EP matrix with a mass ratio of 5 : 2, which is 60.0% and 11.5% lower than pure EP. The above results indicate that the synergistic system of NiPS and MFAPP can reduce the heat release during the combustion of EP composites significantly. The release of large quantities of toxic and hazardous smokes in the event of a fire is a significant factor in the loss of life. The PSPR and TSP of pure EP are 0.56 m^2 s^{-1} and 99.3 m^2, respectively. The PSPR and TSP of EP/5.7MFAPP/2.3NiPS are 0.37 m^2 s^{-1} and 79.5 m^2, respectively, which is 33.9% and 22.0% lower than pure EP. The peak CO release curves of EP/5.7MFAPP/2.3NiPS is lower than those of

pure EP as can be seen in Fig. 2e. The above results show that the synergistic system of MFAPP and NiPS can inhibit the smoke release effectively during the combustion of EP composites. It can be seen in Fig. 2f that the residual char of EP/5.7MFAPP/2.3NiPS is as high as 24.9%, which is much higher than that of pure EP at 1.72%, indicating that the synergistic effect of MFAPP and NiPS promotes the generation of residual char.

FPI is the ratio of ignition time TTI to PHRR and is used to evaluate the flame retardancy of the material, the larger the value, the higher the flame retardancy of the material. The FGI index refers to the ratio of the peak heat release rate to the time required to reach PHRR, the larger the FGI value, the higher the fire hazard factor.[17,18] The values of FBI and FGI for pure EP are 0.03 and 12.68, respectively, while EP/5.7MFAPP/2.3NiPS are
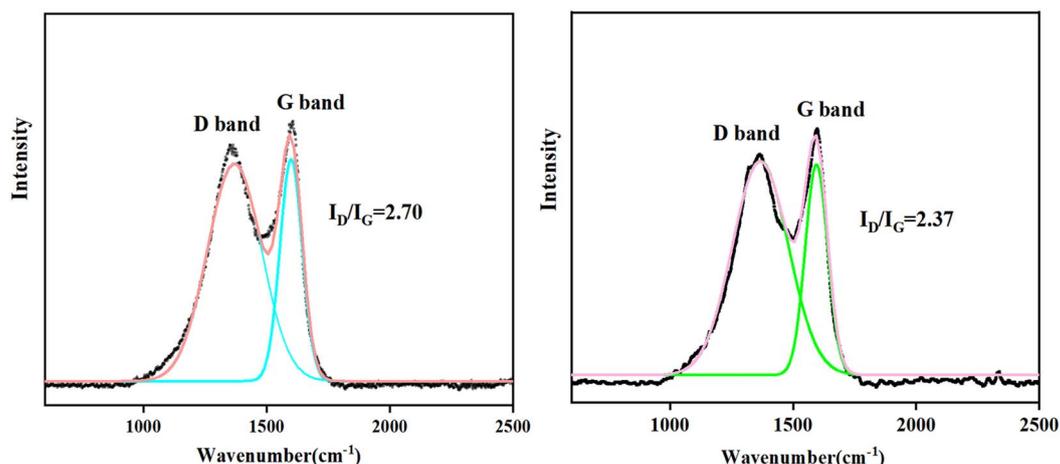

Fig. 4 Raman spectra of the residual chars of pure EP (a) and EP/5.7MFAPP/2.3NiPS (b).

12.68 and 4.31, and the comparison shows that the synergistic effect of NiPS and MFAPP can reduce the fire hazard of EP composites significantly.

3.3. The analysis on residual char

The electron photographs of the residual char morphology of EP and EP composite are shown in Fig. 3. Pure EP shows a broken char layer, and the EP is burned out essentially. The EP/5.7MFAPP/2.3NiPS generates an expanded char layer of about 6 cm in height after combustion, with some green substances adhering to the surface of the char layer, and it can be seen that the surface of the residual char is relatively dense.

This dense and expanded char layer structure can play a physical barrier role in blocking the transmission of heat and combustible gases at high temperatures, protecting the underlying matrix and improving the flame retardancy of the composite.[19]

Raman spectroscopy is used to analyze the graphitization degree of the residual char. There are two peaks at about 1350 cm^{-1} and 1570 cm^{-1}, corresponding to the D band and the G band in Fig. 4, respectively. The value of I_D/I_G is used to show the degree of graphitization, and the lower the I_D/I_G value, the higher the degree of graphitization is indicated.[20] The I_D/I_G value of pure EP is 2.70, while the I_D/I_G value of EP/5MFAPP/2NiPS is 2.37, indicating that a higher degree of graphitization and the formation of a more stable carbon structure. Carbonaceous microstructure with a higher degree of graphitization indicates better thermal stability and stronger residual char residue, which is beneficial for improving flame retardancy and smoke suppression effects.

3.4. Thermal stability of EP composites

Fig. 5 shows the TGA and DTG curves of EP composites under nitrogen atmosphere, and the relevant parameters are listed in Table 3. T_i is the initial decomposition temperature, T_{max} represents the maximum temperature at which the maximum decomposition rate is obtained, R_{max} is defined as the maximum weight loss rate, and char is the residual char rate at

Table 3 Thermal stability parameters for pure EP and composites

Samples	T_i (°C)	T_{max} (°C)	R_{max} (% °C^{-1})	Char (%)
Pure EP	359.2	388.1	2.1	11.7
EP/7MFAPP	319.4	359.7	1.2	27.8
EP/7NiPS	346.2	383.1	1.5	12.0
EP/6MFAPP/1NiPS	296.1	387.9	1.4	22.7
EP/5MFAPP/2NiPS	303.7	384.3	0.7	28.9
EP/4MFAPP/3NiPS	336.4	386.9	1.0	21.6
EP/5.7MFAPP/2.3NiPS	300.2	383.8	0.7	30.1

700 °C. The thermal decomposition process of EP composites under N$_2$ atmosphere is a first order reaction, thermal weight loss is mainly due to thermal degradation of the macromolecular chains in the EP structure.[21] The T_i of pure EP is 359.2 °C, T_{max} is 388.1 °C, R_{max} is 2.1% °C^{-1}, and the residual char rate at 700 °C is only 11.7%. When 7 wt% MFAPP is added, T_i, T_{max}, and R_{max} of EP composite decrease to 319.4 °C, 359.7 °C, and 1.2% °C^{-1}, respectively, while the residual char rate increases to 27.8%. When 7 wt% NiPS is added, T_i and T_{max} is 346.2 °C and 383.1 °C, respectively, R_{max} is 1.5% °C^{-1}, and the residual char rate is 12.0%. The T_i of EP/6MFAPP/1NiPS is greatly reduced to 298.1 °C, R_{max} is reduced to 1.4% °C^{-1}, and the residual char rate is 22.7%. The T_i, T_{max}, and R_{max} of EP/5MFAPP/2NiPS are reduce to 303.7 °C, 384.3 °C, and 0.7% °C^{-1}, and the residual char rate increases to 28.9%. When MFAPP : NiPS is 4 : 3, T_i is 336.4 °C, and T_{max} is 386.9 °C, the residual char rate is 21.6%. Compared with EP/5MFAPP/2NiPS, EP/5.7MFAPP/2.3NiPS shows a slightly lower T_i and T_{max}, while the residual char rate increased by 1.2%, indicating that the residual char rate increases with the addition of MFAPP and NiPS.

The addition of MFAPP and NiPS causes the T_i and T_{max} of EP composites shift to low temperature, and the residual char rate shows different degrees of increase, indicating that the synergistic effect of NiPS and MFAPP can promote the thermal decomposition of EP. This is mainly due to the fact that MFAPP tends to decompose prematurely to produce phosphoric acid and its derivative dehydrating agents, which promotes the
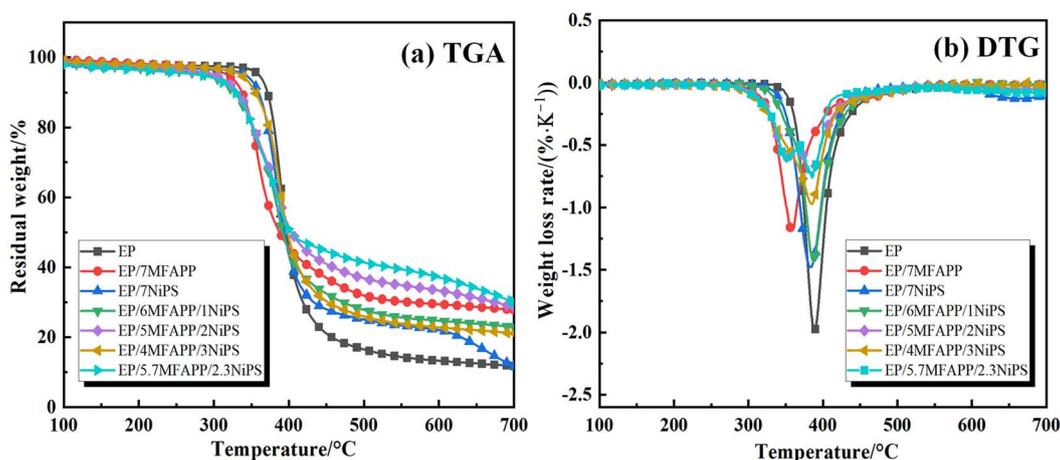

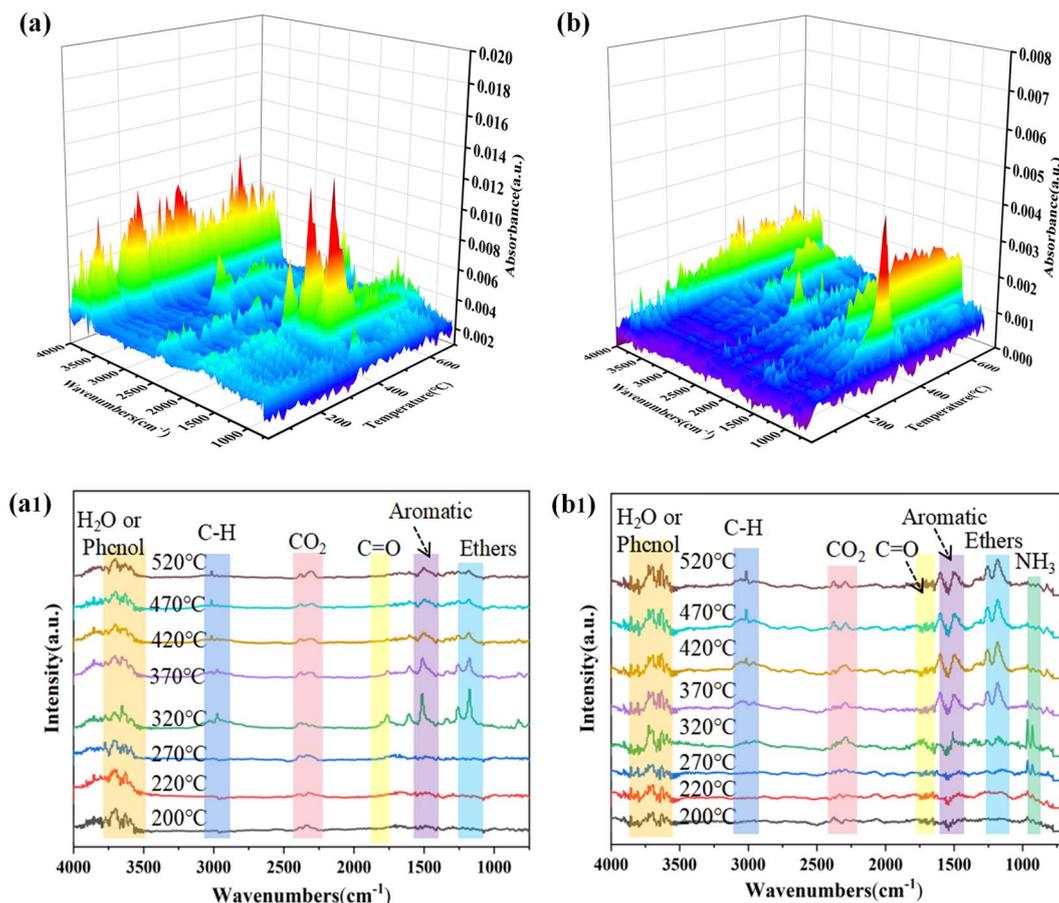**Fig. 5** TGA and DTG results for pure EP and composites under N$_2$ atmosphere.

Fig. 6 Three-dimensional FTIR spectra of the pyrolytic volatile products of EP (a) and EP/5.7MFAPP/2.3NiPS (b); FTIR spectra of pyrolysis products at different decomposition temperatures of EP (a_1) and EP/5.7MFAPP/2.3NiPS (b_1).

premature dehydration of EP to generate a protective char layer, the addition of NiPS may promote the early decomposition of MFAPP,[22] exacerbating the dehydration and carbonization of EP. In summary, when the ratio of MFAPP to NiPS was 5 : 2, the EP composite has the lowest R_{max} and the highest residual char rate, which is better than the residual char rate of MFAPP or NiPS alone at the same additive amount, indicating that there is a better synergistic effect between MFAPP and NiPS at this ratio.

3.5. Analysis of pyrolysis gases and exploration of the mechanism

TG-IR was utilized to identify the pyrolytic volatile products of the pure EP and EP/5.7MFAPP/2.3NiPS during the thermal decomposition process. The 3D IR spectra of the gaseous phase during the thermal degradation of EP and its composites are shown in Fig. 6(a and b), which allows a visual comparison of the differences in the intensity of the gaseous products from the decomposition of the two. The peak intensity of EP/5.7MFAPP/2.3NiPS are generally weaker than those of pure EP, suggesting that NiPS and MFAPP influenced the volatile products generated by thermal cracking of the EP matrix. It can be seen that pure EP decomposes from about 320 °C, and the main gaseous products are compounds containing –OH groups (e.g., water,

phenol; 3500–4000 cm^{-1}), alkanes (2800–3100 cm^{-1}), carbon dioxide (2360 cm^{-1}), carbonyl-based compounds (1650–1850 cm^{-1}), aromatic hydrocarbons (1250–1610 cm^{-1}), ethers (1110–1220 cm^{-1}).[23–26] The EP/5.7MFAPP/2.3NiPS has a lower decomposition temperature than pure EP. At 270 °C, NH$_3$ absorption peak (968 928 cm^{-1}) can be detected. As the temperature increases to 320 °C, vibrations of the P–O bond are detected at 880 cm^{-1} and 1070 cm^{-1}, and vibrations of the P=O bond are detected at 1253 cm^{-1}. The P–O and P=O bonds can capture OH˙ or H˙ radicals effectively in the gas phase, playing a flame-retardant role.[27,28]

To further investigate the variation of the EP pyrolysis products, the absorption intensity versus time curves of several typical volatile products are given, and the corresponding results are shown in Fig. 7. The intensity of the absorption peaks of ethers, aromatic compounds, saturated hydrocarbons and unsaturated hydrocarbons from EP composite is significantly weaker than that of pure EP. In a fire accident, the hydrocarbons and aromatic compounds released by the heat of the material can be used as fuel to participate in the continuation of combustion, and will form toxic and harmful smokes, increasing the risk of fire.[23] Therefore, the reduction in the release of ethers, aromatics, saturated and unsaturated
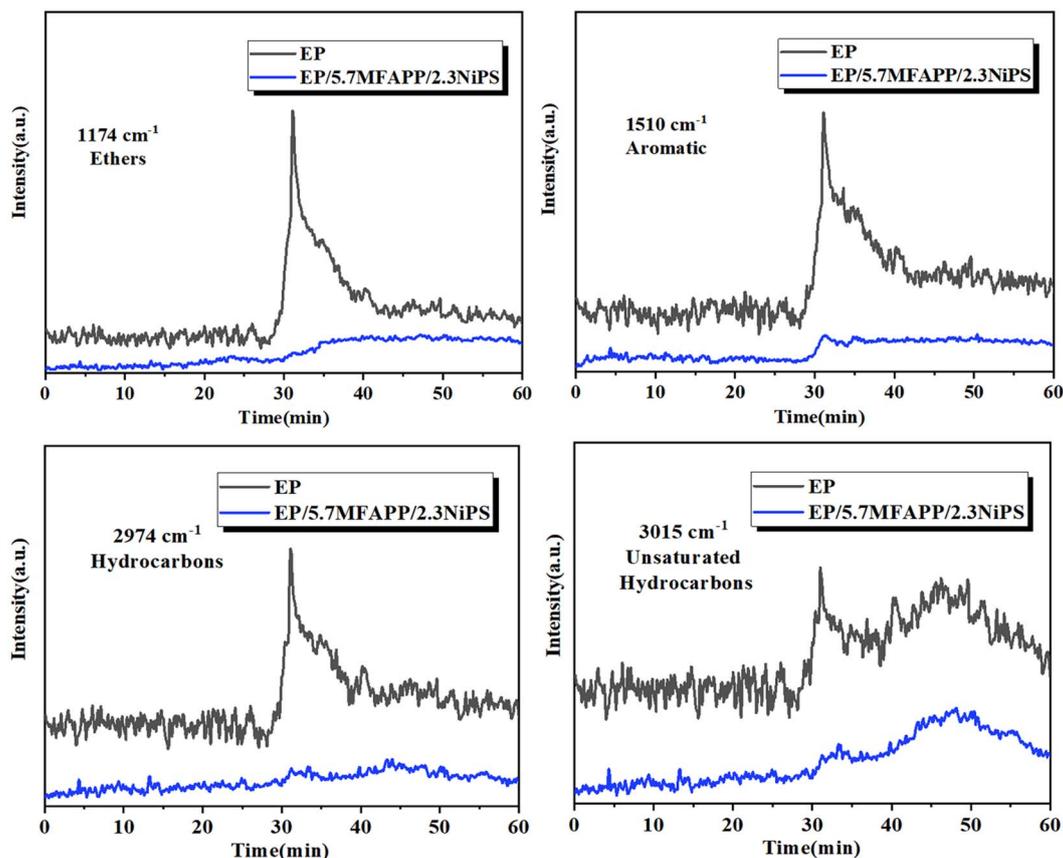
Fig. 7 Ethers, aromatic, carbonyl, hydrocarbons and unsaturated hydrocarbons release profiles for EP and EP/5.7MFAPP/2.3NiPS.

hydrocarbons during the pyrolysis of EP/5.7MFAPP/2.3NiPS further indicates that the composite has better fire safety.

3.6. Tribological performances

The tribological properties of EP composites were investigated using the friction testing machine under dry sliding conditions. Fig. 8a shows the friction coefficient *versus* friction time curves of EP composites under dry friction, and it can be found that the

curves of all EP composites tend to be flat from fluctuations significantly. The whole friction process of EP composites can be divided into two stages, I (running-in) and II (steady state). In stage I, due to the rapid increase in real contact area and the inability to form the transfer film between the EP composites and the steel friction ring, the friction coefficient curves show significant fluctuations. In stage II, the effective transfer film is formed, resulting in a steady state.[29,30] In the NiPS and MFAPP
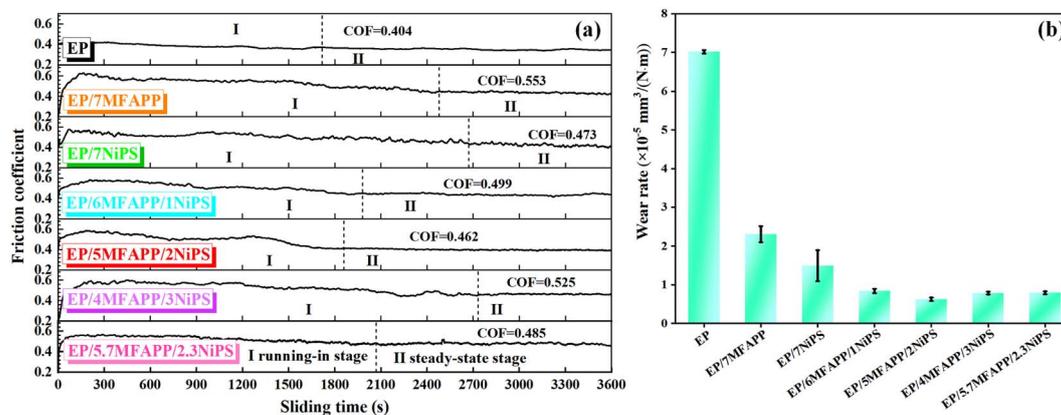

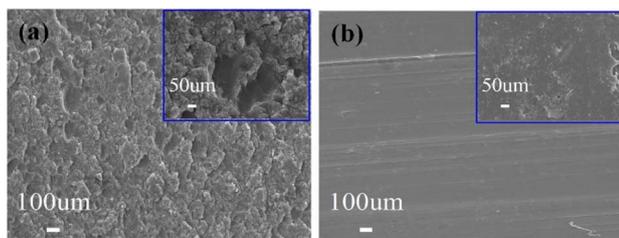Fig. 8 Friction coefficient curves (a) and the wear rate (b) of EP composites.

Fig. 9 SEM of worn surfaces for the (a) EP and (b) EP/2.3NiPS/5.7MFAPP.

synergistic system, the running-in time of EP composites decreases slightly, but it still remains higher than that of pure EP. The coefficient of friction (COF) of all EP composites are higher than that of pure EP, due to the presence of rigid inorganic fillers that rough up the surface in contact with the friction sub.[31]

Fig. 8b shows the wear rate of EP composites. Pure EP has the highest wear rate of 7.03×10^{-5} mm^3 (N^{-1} m^{-1}), indicating its poor anti-wear performance.[32] The wear rates of EP/7MFAPP and EP/7NiPS are 2.3×10^{-5} mm^3 (N^{-1} m^{-1}) and 1.50×10^{-5} mm^3 (N^{-1} m^{-1}) respectively, showing a decrease compared to pure EP. However, the wear rate of EP/5MFAPP/2NiPS is just

0.63×10^{-5} mm^3 (N^{-1} m^{-1}), which is significantly lower than pure EP and the addition of MFAPP or NiPS alone. It can be observed that the wear rate influenced by the ratio of MFAPP or NiPS, the best ratio is 5 : 2. The wear rate of EP/5.7MFAPP/2.3NiPS with excellent flame retardant effect is 0.85×10^{-5} mm^3 (N^{-1} m^{-1}), which is 86.7% lower than that of pure EP, indicating that the EP composites prepared under this system has both excellent flame retardant and wear resistance properties.

The wear surface of the EP composites was further observed using SEM, and the results are shown in Fig. 9. The pure EP has more obvious traces of flake shedding and a rough surface, and the main wear mechanisms are fatigue wear and adhesive wear.[33,34] Under the action of periodic frictional forces, some resin fragments were dislodged, and the dislodged fragments were transferred to the steel friction ring surface during the bonding process, increasing the actual contact area and intensifying the wear. On the other hand, when cracks accumulated on the surface of EP and exceeded the critical value, it led to fatigue wear accompanied by significant abrasive loss.[33,34] The wear surface of EP/5.7MFAPP/2.3NiPS is relatively flat, without significant brittle tearing fragments, only a small amount of plowing and grooving. This phenomenon indicates that the addition of MFAPP and NiPS can change the wear mode of the
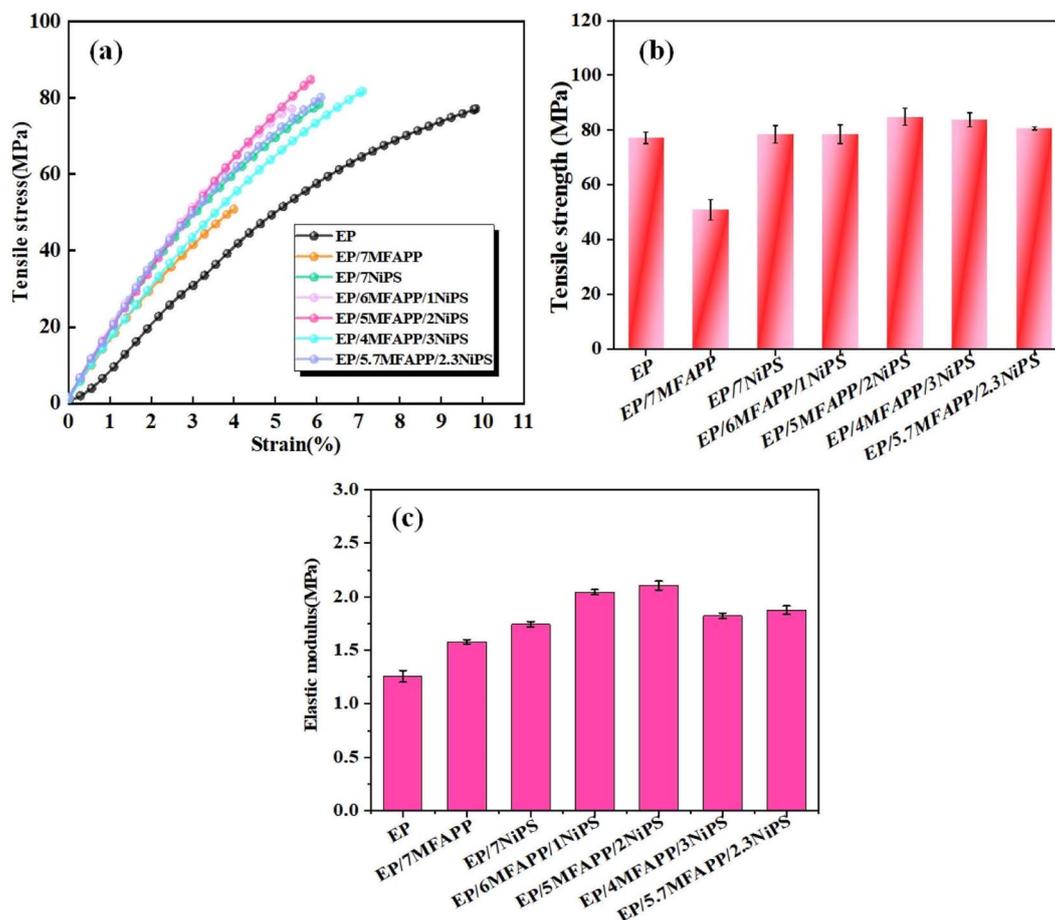

Fig. 10 Mechanical properties of investigated samples: (a) tensile stress–strain curves, (b) tensile strength and (c) elastic modulus.

EP composite, reducing adhesive wear and fatigue delamination significantly, abrasive wear becomes the main wear mechanism, causing wear through cutting. Whereas the abrasive wear shall give a major contribution to the significantly enhanced anti-wear properties of EP composites.[35,36]

3.7. Mechanical properties

In order to investigate the influence of the synergistic effect of MFAPP and NiPS on the mechanical properties of EP composites, quasi-static tensile tests are performed, and the results are shown in Fig. 10. Fig. 10a presents the stress–strain curves of the composites, which exhibits a brittle behavior without a distinct yield plateau before failure. Fig. 10b shows that the tensile strength of pure EP is 78.2 MPa, while it decreases significantly to 48.0 MPa when 7 wt% MFAPP is added, indicating a substantial damage to the mechanical properties caused by the addition of MFAPP alone. The tensile strength of EP/7NiPS is 80.4 MPa, which increases by 2.2 MPa compared to pure EP. However, it is lower than the tensile strength of EP composite with the addition of 3 wt% NiPS in our previously reported article, this can be attributed to the fact that excess inorganic fillers tend to aggregate and act as mechanical defects in EP composites, weakening the enhancement effect.[14,37]

The tensile strength of EP composites in the synergistic system of NiPS and MFAPP increases first and then decreases with the increase of NiPS content. Among them, the EP/5MFAPP/2NiPS exhibits the highest tensile strength of 86.0 MPa, which is an improvement of 7.8 MPa compared to pure EP. From Fig. 10c, it can be seen that the EP composites show higher modulus of elasticity, the elastic modulus of EP/5MFAPP/2NiPS is 2.10 GPa, which is 1.44 GPa higher than that of pure EP. The EP/5.7MFAPP/2.3NiPS with excellent flame retardancy and friction performance has a tensile strength of 80.6 MPa and an elastic modulus of 1.88 GPa. The tensile strength and modulus of elasticity of the EP composites in this study increased slightly compared to similar articles reported previously.[38] The synergistic effect of MFAPP and NiPS improves the damage to the mechanical properties of EP composites caused by the excessive addition of flame retardants, and achieves a better balance between flame retardant properties and mechanical properties.

4. Conclusion

In order to further improve the flame retardancy and wear resistance of EP composites, this study synthesized NiPS using rod-like Ni-MOFs as the hard template and Ni source template. By synergistic effect with MFAPP, highly efficient flame retardant and wear-resistant EP composites were prepared. The influence of MFAPP and NiPS on the flammable, tribological and friction mechanical performances of EP composites were investigated.

The results showed that at a total addition of 8 wt% and a NiPS : MFAPP mass ratio of 2 : 5, the LOI of EP composite was 28.2%, which could reach the V-0 grade in UL-94. Compared with pure EP, the peak heat release rate and total heat release of EP composite were reduced by 33.9% and 22%, and the peak smoke release rate and total heat release were reduced by 66.2% and 11.5%, indicating that EP composite have more excellent flame retardant and smoke suppression performance.

The synergistic system of NiPS and MFAPP promoted the production of high quality char layer, which was denser and more complete, and preventing the diffusion of heat, oxygen and combustible gases during the combustion of EP composites. Meanwhile, MFAPP generated phosphorus-containing functional groups at high temperature to trap OH$^\bullet$ or H$^\bullet$ radicals in the gas phase, which could interrupt the combustion chain reaction of EP composite and inhibit the combustion behavior.

Dry friction experiments showed that the synergy of NiPS and MFAPP was beneficial to improve the wear resistance of EP composites. The mass wear rate of EP/5.7MFAPP/2.3NiPS was 0.847×10^{-5} mm^3 N^{-1} m^{-1}, which was 87.6% lower than that of pure EP. In addition, the mechanical properties of the EP composites were improved, showing high tensile strength and elastic modulus.

Conflicts of interest

The authors declare that they have no known competing financial interests or personal relationships that could have appeared to influence the work reported in this paper.

Acknowledgements

References

1 E. Esmizadeh, G. Naderi, A. A. Yousefi and C. Milone, *J. Therm. Anal. Calorim.*, 2016, **126**, 771–784.

2 J. T. Luo, S. R. Yang, L. Q. Lei, J. Q. Zhao and Z. Tong, *Composites, Part A*, 2017, **100**, 275–284.

3 Y. J. Xue, M. X. Shen, S. H. Zeng, W. Zhang, L. Y. Hao, L. Yang and P. A. Song, *Mater. Res. Express*, 2019, **6**, 12.

4 S. Sasidharan and A. Anand, *Ind. Eng. Chem. Res.*, 2020, **59**, 15.

5 H. Y. Wei, J. Xia, W. L. Zhou, L. S. Zhou, G. Hussain, Q. Li and K. Ostrikov, *Composites, Part B*, 2020, **193**, 20.

6 U. O. Uyor, A. P. I. Popoola, O. M. Popoola and V. S. Aigbodion, *J. Thermoplast. Compos. Mater.*, 2020, **33**, 1030–1047.

7 C. Wang, Z. G. Xie, K. E. deKrafft and W. L. Lin, *J. Am. Chem. Soc.*, 2011, **133**, 13445–13454.

8 C. Li, j. T. Wan, E. N. Kalall, H. Fan and D. Y. Wang, *J. Mater. Chem. A*, 2015, **3**, 3471–3479.

9 Z. Li, Z. Q. Liu, F. Dufosse, L. K. Yan and D. Y. Wang, *Composites, Part B*, 2018, **152**, 336–346.

10 H. Y. Wang, L. Yan, D. J. Liu, C. Wang and J. H. Zhu, *Tribol. Int.*, 2015, **83**, 139–145.

11 J. Song, Z. D. Dai, J. Y. Li, H. C. Zhao and L. P. Wang, *High Perform. Polym.*, 2019, **31**, 116–123.

12 Z. F. Bian and S. Kawi, *Catal. Today*, 2020, **339**, 3–23.

13 J. N. Yang, Z. Y. Li, Y. X. Xu, S. B. Nie and Y. Liu, *J. Polym. Res.*, 2020, **27**, 14.

14 Y. X. Xu, G. L. Dai, S. B. Nie, J. N. Yang, S. Liu, H. Zhang and X. Dong, *Front. Chem. Sci. Eng.*, 2022, **16**, 1493–1504.

15 J. N. Yang, Y. Liu, Y. X. Xu, S. B. Nie and Z. Y. Li, *J. Mater. Sci.*, 2020, **55**, 10593–10610.

16 Z. T. Liu, M. Q. Dai, Q. H. Hu, S. Liu, X. Gao, F. Ren and Q. Zhang, *J. Coat. Technol. Res.*, 2019, **16**, 135–145.

17 Y. H. Jiao, X. L. Wang, Y. Z. Wang, D. Y. Wang, Y. L. Zhai and J. S. Lin, *J. Macromol. Sci., Part B: Phys.*, 2009, **48**, 889–909.

18 B. R. Duan, Q. J. Wang, X. Wang, Y. Li, M. M. Zhang and S. Diao, *Results Phys.*, 2019, **15**, 5.

19 A. Klingler and B. Wetzel, *Polym. Eng. Sci.*, 2017, **57**, 579–587.

20 A. J. Li, W. Z. Xu, R. Chen, Y. C. Liu and W. Li, *Composites, Part A*, 2018, **112**, 558–571.

21 A. M. Pinto and F. D. Magalhaes, *Polymers*, 2021, **13**, 5.

22 K. Wu, L. Song, Z. Z. Wang, Y. Hu, E. Kandare and B. K. Kandola, *J. Macromol. Sci., Part A: Pure Appl.Chem.*, 2009, **46**, 837–846.

23 Y. L. Sui, L. J. Qu, X. Y. Dai, P. H. Li, J. R. Zhang, S. Luo and C. L. Zhang, *RSC Adv.*, 2020, **10**, 12492–12503.

24 Z. Q. Xiong, Y. Zhang, X. Y. Du, P. A. Song and Z. P. Fang, *ACS Sustain. Chem. Eng.*, 2019, **7**, 8954–8963.

25 J. Zhang, Z. Li, X. L. Qi, W. Zhang and D. Y. Wang, *Composites, Part B*, 2020, **188**, 10.

26 Y. Zheng, Y. S. Lu and K. Q. Zhou, *J. Therm. Anal. Calorim.*, 2019, **138**, 905–914.

27 Y. B. Hou, L. X. Liu, S. L. Qiu, X. Zhou, Z. Gui and Y. Hu, *ACS Appl. Mater. Interfaces*, 2018, **10**, 8274–8286.

28 X. Xu, R. Cao, S. Jeong and J. Cho, *Nano Lett.*, 2012, **12**, 4988–4991.

29 S. Gupta, T. Hammann, R. Johnson and M. F. Riyad, *Tribol. Trans.*, 2015, **58**, 560–566.

30 N. Myshkin and A. Kovalev, *Friction*, 2018, **6**, 143–155.

31 R. Baptista, A. Mendao, F. Rodrigues, C. G. Figueiredo-Pina, M. Guedes and R. Marat-Mendes, *Theor. Appl. Fract. Mech.*, 2016, **85**, 113–124.

32 J. S. Chen, J. Yang, B. B. Chen, S. Liu, J. Z. Dong and C. S. Li, *Surf. Coat. Technol.*, 2016, **305**, 23–28.

33 A. Dasari, Z. Z. Yu and Y. W. Mai, *Mater. Sci. Eng., R*, 2009, **63**, 31–80.

34 M. M. Sakka, Z. Antar, K. Elleuch and J. F. Feller, *Friction*, 2017, **5**, 171–182.

35 S. L. Fu, X. H. Chen, P. Liu, H. P. Cui, H. L. Zhou, F. C. Ma and W. Li, *J. Mater. Eng. Perform.*, 2022, **31**, 4955–4962.

36 M. S. Zhang, B. B. Chen, H. Tang, G. G. Tang, C. S. Li, L. Chen, H. M. Zhang and Q. Zhang, *RSC Adv.*, 2015, **5**, 1417–1423.

37 X. Y. Ma and W. D. Zhang, *Polym. Degrad. Stab.*, 2009, **94**, 1103–1109.

38 J. Lin, K. Q. Wang, J. G. Li, D. S. Yang, Y. Y. Zhu and X. L. Wang, *J. Mater. Sci.*, 2021, **56**, 19899–19914.